

XVII International Colloquium on Mechanical Fatigue of Metals (ICMFM17)

Analysis of cyclic plastic response of heat resistant Sanicro 25 steel at ambient and elevated temperatures

Jaroslav Polák^{a,b,*}, Roman Petráš^a, Milan Heczko^a, Tomáš Kruml^{a,b}, Guocai Chai^{c,d}

^a*Institute of Physics of Materials, Academy of Sciences of the Czech Republic, Brno, 623 00, Czech Republic*

^b*CEITEC, Institute of Physics of Materials, Academy of Sciences of the Czech Republic, Brno, 623 00, Czech Republic*

^c*Sandvik Materials Technology, SE-811 81 Sandviken, Sweden*

^d*Linköping University, Engineering materials, SE-581 83 Linköping, Sweden*

Abstract

Austenitic heat resistant steel Sanicro 25 developed for high temperature applications in power generation industry has been subjected to selected low cycle fatigue tests at ambient and at elevated temperature. Saturated hysteresis loops at both temperatures were analyzed to deduce the probability density distribution of the internal critical stresses and to estimate the contribution of the effective stress for different strain amplitudes. The internal structure of the material at room and elevated temperature was studied using transmission electron microscopy and the results were discussed in relation to the cyclic stress-strain response

© 2014 Elsevier Ltd. Open access under [CC BY-NC-ND license](https://creativecommons.org/licenses/by-nc-nd/4.0/).

Selection and peer-review under responsibility of the Politecnico di Milano, Dipartimento di Meccanica

Keywords: heat resistant steel, Sanicro 25, cyclic plasticity, dislocation structure, effect of temperature

1. Introduction

Austenitic stainless steel Sandvik Sanicro 25 has been developed for applications at elevated temperatures, namely for construction of supercritical boilers [1,2]. Mostly creep behavior and high temperature corrosion and to a certain extent also low cycle fatigue properties were studied [2]. The present paper is devoted to the comparison of the cyclic stress-strain behavior at ambient and at elevated temperature and to the study of dislocation arrangement produced by cyclic straining at ambient and elevated temperatures.

* Corresponding author. Jaroslav Polak Tel.: +420-532-290-366; fax: +420-541-218-657.

E-mail address: polak@ipm.cz

2. Experimental

Experimental material was supplied by Sandvik, Sweden in the form of the cylindrical rod of 150 mm in diameter. The chemical composition of the material can be found elsewhere [2]. Cylindrical specimens for cyclic straining at room and elevated temperatures were machined with the axis parallel to the rod. The gauge length and diameter of specimens were 14 mm and 8mm respectively for room temperature testing and 15mm and 6 mm for elevated temperature testing. Specimens were homogenized at 1200 °C for 10 minutes and cooled in air. Afterwards final grinding was done.

Cyclic straining was performed in computer-controlled electrohydraulic MTS system. Constant strain rate $5 \times 10^{-3} \text{ s}^{-1}$ was applied at room temperature and $2 \times 10^{-3} \text{ s}^{-1}$ at temperature 700 °C. High number of data points was recorded for each hysteresis loop. Hysteresis half-loops in relative coordinates were smoothed and digitally differentiated and the first and second derivatives of both tensile and compressive half-loops could be obtained in agreement with the statistical theory of the hysteresis loop [3]. The section of the plot of the second derivative vs. fictive stress corresponding to the probability density function of the internal critical stresses was fitted by the Weibull function.

Thin foils for the transmission electron microscopy were prepared using standard procedures from sections taken at 45 degrees to the specimen axis. They were studied in a transmission electron microscope STEM Philips CM-12 operating at 120 kV using a double tilt holder and a MegaView II digital camera.

3. Results

Fig. 1 shows the plot of the stress amplitude vs. number of cycles during several blocks of constant strain amplitude loading with suddenly increasing total strain amplitude at room temperature and at temperature 700 °C. Number of cycles at each level N_i was inversely proportional to the applied total strain amplitude ϵ_{ai} so that $N_i \epsilon_{ai} = 20$. Room temperature cycling results in cyclic softening at all strain levels. When the strain amplitude suddenly increases, the stress amplitude increases too but later cycling leads to cyclic softening. Identical cyclic straining at temperature 700 ° results in cyclic hardening at all strain levels. In both cases the saturated levels of the stress amplitude were not achieved and thus the final data points cannot be used for the construction of the cyclic stress-strain curve.

Hysteresis loops recorded at the end of each block of strain amplitudes are plotted in relative coordinates (origin of coordinates of each loop was chosen the minimum strain and stress in each loop) in Fig. 2. The non-Masing behavior, as widely denoted [4], is apparent in cycling at both temperatures. It means that the shape of the smaller hysteresis loops cannot be derived from the shape of the largest hysteresis loop. At room temperature the small loops are higher than the corresponding part of the largest loop and at high temperature the small loop is well below the corresponding part of the largest loop.

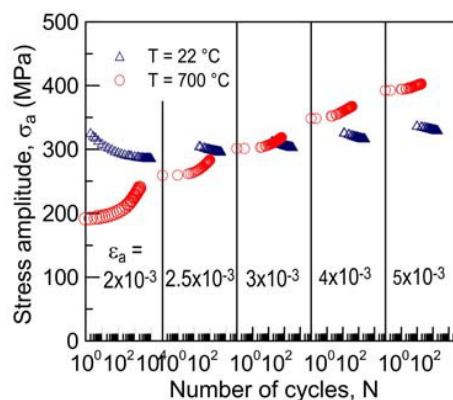


Fig. 1. Stress amplitude vs. number of cycles in loading with increasing strain amplitudes at two temperatures.

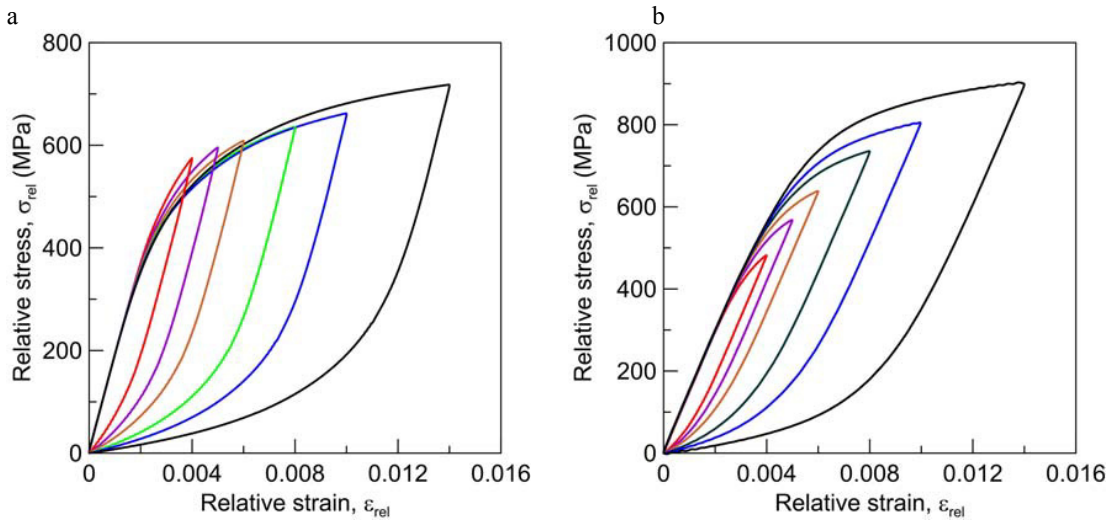


Fig. 2. Hysteresis loops at the end of each block of strain amplitude; a) room temperature cycling, b) cycling at temperature 700 °C.

The probability density distribution of the internal critical stresses at a particular strain amplitude and temperature could be obtained by evaluating second derivative [3,5] of the hysteresis half loop using relation

$$f\left(\frac{\varepsilon_r E_{eff}}{2} - \sigma_{es}\right) = -\frac{2}{E_{eff}^2} \frac{\partial^2 \sigma_r}{\partial \varepsilon_r^2} \quad (1)$$

where ε_r and σ_r are relative coordinates of the particular half-loop. E_{eff} is the effective elastic modulus derived from the respective hysteresis half-loop and σ_{es} is the saturated effective stress. Relation (1) shows that by plotting the second derivative of the hysteresis half-loop (multiplied by $-2/E_{eff}^2$) vs. fictive stress $\varepsilon_r E_{eff}/2$ we can evaluate the saturated effective stress from the offset of the peak of the probability density function relative to the origin.

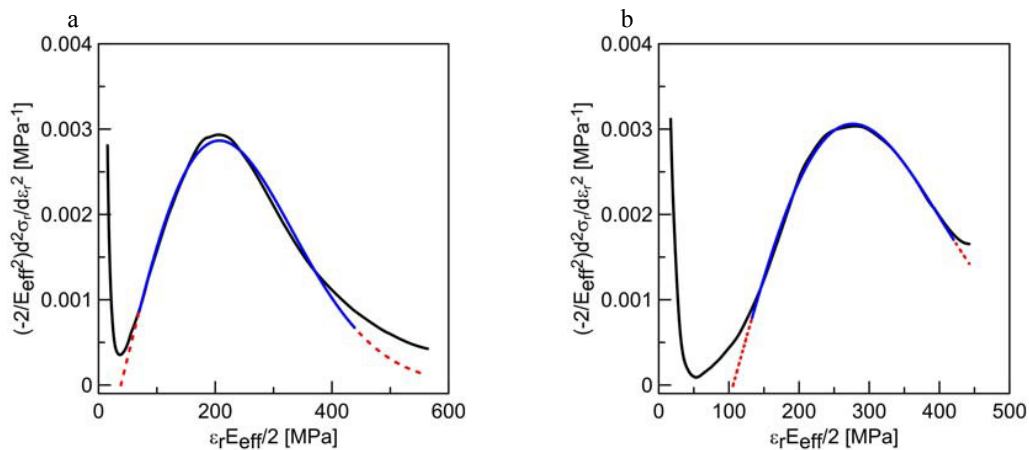


Fig. 3. Second derivative of the tensile hysteresis half-loop in cycling with strain amplitude 3×10^{-3} ; a) room temperature cycling, b) cycling at temperature 700 °C.

Fig. 3 shows the second derivatives of the hysteresis half-loops at two temperatures. Since effective elastic modulus at 700 °C is much lower (130 GPa) than at room temperature (200 GPa) the fictive stress in Fig. 3b (x axis) extends to lower values than in Fig. 3a. The initial part of the plot the second derivative is steeply decreasing which corresponds to the rapid relaxation of the effective stress during unloading from maximum compression. The major part corresponds to the probability density function of the internal critical stresses $f(\sigma_{ic})$.

In order to evaluate the saturated effective stress σ_{es} in agreement with eq. (1) and analytically approximate the shape of the probability density distribution we have used only the data around the peak of the second derivative and they were approximated by the translated Weibull distribution in the form

$$f(x) = \frac{b}{a} \left(\frac{x-d}{a} \right)^{b-1} \exp \left[- \left(\frac{x-d}{a} \right)^b \right] \quad (2)$$

where a is scale parameter, b the shape parameter and d the location parameter. d is equal to the saturated effective stress σ_{es} (see eq. (1)). All three parameters were evaluated for all tensile hysteresis loops from the experimental data using least squares fitting procedure. The shape parameter was always very close to the 2 and therefore in further analysis it was fixed and all fitting were done again with $b = 2$.

Table 1 shows the parameters a , b and $d = \sigma_{es}$ for both temperatures simultaneously with the $(\varepsilon_r E_{eff}/2)_M$ and fictive stress σ_{fM} corresponding to the maximum of the probability density function.

Fig. 4 shows the typical dislocation arrangement in the grains of the Sanicro 25 fatigued to fracture at two temperatures with the strain amplitude 3.5×10^{-3} . Dislocation arrangement in a foil prepared from specimen cycled at room temperature (Fig. 4a) shows thin parallel dislocation rich bands which alternate with areas nearly free of dislocations. The bands run parallel with the trace of (111) slip plane. This arrangement corresponds to the starting localization of the cyclic plastic strain in a particular grain. Dislocation density in the grain from the specimen cycled at 700 °C (Fig. 4b) is much higher. The individual bands parallel to the trace of primary slip plane are also visible; however, high dislocation density is present also in between these bands.

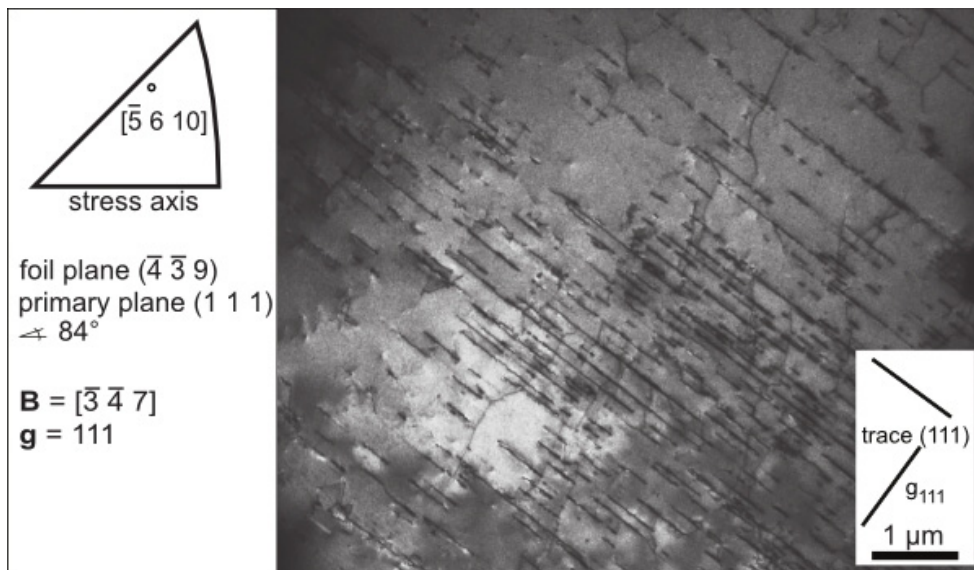


Fig. 4. Dislocation structure in grains from specimens cycled at temperature 22 °C with strain amplitude 3.5×10^{-3} to fracture.

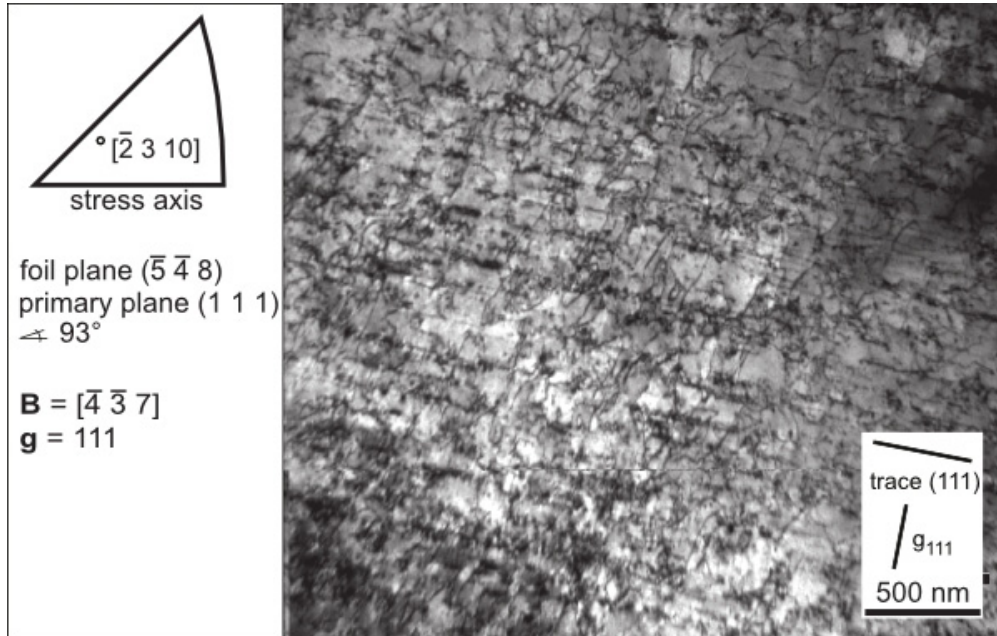


Fig. 5. Dislocation structure in grains from specimens cycled at temperature 700 °C with strain amplitude 3.5×10^{-3} to fracture.

Table 1. Parameters of the Weibull distribution fitted to the upper part (y coordinate higher than 50% of peak value) of the plot of the second derivative versus $\varepsilon_r E_{eff}/2$ for two temperatures.

T (°C)	a (MPa)	b	$d = \sigma_{es}$ (MPa)	$(\varepsilon_r E_{eff}/2)_M$ (MPa)	σ_M (MPa)
22	239	2	38	207	169
700	241	2	106	276	170

4. Discussion

The cyclic plastic response of the Sanicro 25 steel at room and at elevated temperature is substantially different. Room temperature cyclic straining leads to cyclic softening while cyclic straining at temperature 700°C results in appreciable cyclic hardening. The analysis of the hysteresis loop in terms of the effective stress and the distribution of the internal critical stresses of the microvolumes revealed that effective stress at room temperature is low (38 MPa) and still decreases in cyclic straining. This decrease is due to the increase of the density of mobile dislocations (dislocation loops) due to localization of the cyclic plastic strain in the bands of stable cyclic slip - persistent slip bands. To compensate the increase of the mobile dislocations their velocity decreases which is connected with the decrease of the effective stress. This conclusion is in accord with the dislocation arrangement found after room temperature cyclic straining (Fig. 5a) which corresponds to the formation of multiple parallel bands. Mobile dislocations stay mostly in primary plane and multiple annihilation of dislocations takes place during cyclic straining. Some of these bands could become persistent slip bands.

The cyclic hardening of Sanicro 25 steel at temperature 700 °C is due to interaction of the dislocations with nanoclusters observed in this material earlier [2] and also here. The nanoclusters are hardly to distinguish in the image shown in Fig. 5b but higher magnification dark field micrographs show nanoclusters of the average size of 50 nm. The interaction of mobile dislocation loops with nanoclusters leads to cross glide of dislocations and to prevention of the mutual annihilation of dislocations in cyclic straining. Since cross glide at elevated temperature is

easier the dislocation glide also in other systems the primary slip system and their density increases. Cyclic strain is much less localized than in room temperature straining and total dislocation density increases. In spite of that the average mobile dislocation density is low since cyclic strain localization is prevented. In order to reach prescribed strain rate the average dislocation velocity must be high which corresponds to the high effective stress.

High effective stress at temperature 700 °C simultaneously with high dislocation density in secondary glide system which represent resistance to movement of primary dislocations are the principal reasons of the higher cyclic stress-strain response of this steel at elevated temperature in comparison with that at room temperature.

5. Conclusions

Study of the cyclic stress strain response of the Sanicro 25 steel at two temperatures using the analysis of the hysteresis loop shape and the study of dislocation structures led to the following conclusions:

(i) Room temperature cyclic straining leads to cyclic softening while cyclic straining at temperature 700 °C results in cyclic hardening at all applied strain amplitudes.

(ii) Analysis of the hysteresis loop shape led to the separation of the contribution of the effective and internal stresses. The higher stress amplitude at 700 °C compared to room temperature is predominantly due to higher effective stress and increased total dislocation density.

(iii) Cyclic hardening and softening behavior at both temperatures can be discussed in terms of internal dislocation arrangement.

Acknowledgements

The support by the grant No. 13-23652S of GACR and the projects RVO: 68081723 is gratefully acknowledged. This work was realized in CEITEC with research infrastructure supported by the project CZ.1.05/1.1.00/02.0068 financed from European Regional Development Fund.

References

- [1] R. Rautio, S. Bruce, Alloy for ultrasupercritical coal fired boilers, *Advanced Mater. & Processes* 166 (2008) 35–37.
- [2] G. Chai, M. Bostrom, M. Olaison, U. Forsberg, Creep and LCF behaviours of newly developed advanced heat resistant austenitic steels for A-USC, *Procedia Engineering* 55 (2013) 232–239.
- [3] J. Polák, M. Klesnil, The Hysteresis Loop 1. A Statistical Theory. *Fatigue Engng Mater. Struct.* 5 (1982) 19-32.
- [4] R.P. Skelton, H.J. Maier, H.-J. Christ, The Bauschinger effect, Masing model and the Ramberg–Osgood relation for cyclic deformation in metals. *Mater. Sci. Eng. A238* (1997) 377–390.
- [5] J. Polák, M. Klesnil, J. Helešic, The Hysteresis Loop 2. An Analysis of the Loop Shape. *Fatigue. Engng Mater. Struct.* 5 (1982) 33-44.